HEFAT2012
9th International Conference on Heat Transfer, Fluid Mechanics and Thermodynamics
16 – 18 July 2012
Malta

FLOW QUALITY IMPROVEMENT IN A TRANSONIC WIND TUNNEL

Amiri K.* and Soltani M.R.
Department of Aerospace, Sharif University of Technology, Tehran, Iran
E-mail: kaveh_amiri@alum.sharif.edu

ABSTRACT

An originally designed trisonic wind tunnel was upgraded to improve its performance criterion in the transonic regimes. In this research, the test section was modified according to the operational requirements of the existing transonic wind tunnels. Suitable perforated walls were designed, manufactured and installed. The flow in the test section of the wind tunnel with the new test section walls was surveyed for the empty condition, using specially designed long tube static probe and a rake. The rake was used to survey Mach number distribution in the test section. Finally, a 2D model (NACA 0012) and a 3D standard model for the transonic wind tunnels (AGARD-B) were manufactured and tested at various conditions for the purpose of the integral calibration and validation of the tunnel data. Surface pressure distribution along with the force and moment data compared well with the existing data from other tunnels when operated in similar stream conditions.

Keywords: transonic wind tunnel/ perforated wall/ side suction/ standard models/ test section.

NOMENCLATURE

C	[m]	Airfoil chord
D	[m]	Model fuselage diameter
h	[m]	Height of the wind tunnel
L	[m]	Test section length
x/L	[-]	Distance from the entrance of test section over test section length
M	[-]	Mach number
Re	[-]	Reynolds Number
MSD	[m]	Mach number Standard Deviation
α	[deg]	Angle of attack
C_L	[-]	Lift coefficient
C_m	[-]	Pitching moment coefficient
C_p	[-]	Pressure coefficient
C_{DF}	[-]	Forebody drag coefficient

INTRODUCTION

One of the most critical flow regimes encountering flying vehicles is their transonic phase of flight. There are two sets of problems relating to this regime. First, absence of efficient governing rules to predict the flow phenomenon which intensifies the necessity of performing laborious wind tunnel and flight tests. The second one is interaction of the flow over the model with the wind tunnel walls. When a model is inserted in a test section with solid walls in a nearsonic flow, it is probable that the flow in the vicinity of the model region in the test section becomes chocked. Furthermore, the accelerated flow over the model surface will almost always terminate with a normal shock along the model. This normal shock will extend toward the wind tunnel wall and its reflection will interact with the model surface again, a phenomenon that will affect aerodynamics force and moment, considerably.

To solve this problem, adaptive, porous, perforated or combinations of these walls are used to eliminate the boundary layer, shocks and chocking of the flow. Porous walls and specially perforated walls are also used for testing models at high angle of attack in the subsonic wind tunnels; where the governing equations are non-linear.

In order to take advantages of these favorable characteristics of the perforated walls for converting a 60cm*60cm test section wind tunnel that was operating at Mach numbers ranging from 0.4 to 0.75 and 1.4 to 2.5, the tunnel test section walls were changed. The flow field in the newly designed and manufactured test section was surveyed and calibrated to validate the predicted improvements. Furthermore, the pressure distribution at the centerline of the wind tunnel by means of a long tube probe was measured.

After designing and manufacturing the perforated walls, a series of tests were conducted to survey the efficiency of the walls and the side suction system, maximum attainable transonic Mach number, and Mach number distribution in the test section of the wind tunnel with new facilities. All tests were performed for the empty test section condition. The pressure and Mach number distribution in the test section and along the nozzle were measured using a specially designed long tube and rake. In addition, two standard models that were tested in several transonic wing tunnels all over the world and information about their surface pressure distribution, force and moments are available were tested and the data are compared with the existing ones. Further, this information is used as baseline for future tests.

EXPERIMENTAL FACILITIES AND INSTRUMENTATION

Numerous equipments were used in this investigation. All equipments except the wind tunnel were designed and

manufactured specifically for these tests. In the following sections a brief description about a few of these equipments will be presented.

Wind Tunnel

All tests were performed in a wind tunnel with a test section of (60cm (W) * 60cm (H) * 150cm (L)). The tunnel is of open circuit suction type. Two engines that eject their exhaust gases downstream of the test section through ejector systems supply the main circuit power of the tunnel. Side suction is supplied by a smaller engine. Figure 1 shows the schematic of the wind tunnel. Both sidewalls are solid and there are three types of interchangeable upper and lower walls; closed, normal perforated and inclined perforated ones. Two plenum chambers are installed above the upper and lower walls of the tunnel.

The New Walls

To investigate the effects of porosity, hole inclination and side suction on the Mach number distribution along the center line of the test section as well as the maximum achievable Mach number, three types of side walls were designed, manufactured, and tested. The first wall was a closed solid one, which is suitable for subsonic and supersonic tests. The other two walls are perforated and are perforated; normal and inclined ones. For further discussions about the walls and other equipments please see ref [[11],[13]].

PRELIMINARY TESTS

To evaluate the flow field in the test section with the newly implemented walls, two sets of preliminary tests were conducted, empty test section tests and one with a long tube probe. The measured data included Mach number distribution along the centerline of the test section calculated from the long tube rake as well as those calculated from the wall static pressure data. Figure 2 and Figure 3 show variations of the Mach number along the test section for the closed and normal perforated wall cases. Similar data are obtained for the inclined walls too, but are not presented in this paper. As seen from these figures Mach number distribution along the test section is satisfactory for all cases.

These results showed that with the solid side walls, maximum attainable Mach number in the test section of the tunnel is about 0.85, Figure 2 . However, when the normal perforated side walls are installed in the test section, the Mach number was increased to about 0.95, Figure 3 . With the exertion of the side suction, maximum obtained Mach number was about 1.18. The effects of porosity and side suction was optimized when the normal perforated walls were replaced by the 60 degrees slanted hole ones. In this case the maximum attainable Mach number in the test section was increased to 1.25.

For further information, please see references [[11], 13].

STANDARD MODELS

Both static and total pressure distribution along the nozzle and tunnel tests section at various Mach numbers, $0.8 \le M_{\infty} \le 1.2$, were measured. From these data, velocity and Mach number distributions along the test section were calculated [[11]]. In this paper, however, only the results for two standard models, that are tested in various tunnels and their data are used as a baseline, are presented. As mentioned, the tunnel is utilized for 2D and 3D tests. Thus, for this part of the tests a 2D and a 3D model are selected for integral calibration of the tunnel. The following criteria were considered in the selection of these models:

- Compatibility of the model with transonic regime
- Frequency of the reported data
- Diversity of the test conditions
- Similarity of the referenced wind tunnels with the present tunnel, ST2
- Ease of the manufacturing

From the above criteria, NACA 0012 airfoil was selected as the 2D calibration model and AGARD-B as the 3D model.

3D Calibration Model (AGARD-B)

There are several 3D models which have been tested in transonic speeds, ranging from conventional simple rockets to high-tech complicated airplanes such as F-18 and F-22. One of the most popular transonic models which is specifically designed by the AGARD group for calibration of the transonic wind tunnels is called AGARD-B. This model has a delta wing with a span four times its body diameter. The body is of a cylindrical body of revolution with an ogive nose (Figure 4). The designed and manufactured model for the present tunnel has a base diameter of 33.2 mm and blockage ratio of 0.29 percent when set at zero degrees angle of attack. However, one should note that the blockage ratio is usually considered for the highest angle of attack where for the present model is within the limitations indicated in Ref [[2]].

2D Calibration Model (NACA 0012)

Among the 2D models, the most distinguished one is NACA-0012 that has been utilized for calibration purposes in various flow regimes; subsonic, transonic and supersonic ones and many CFD results for all cases are available in the literature. Consequently, there are lots of references that published a vast variety of data from pressure distribution to force and moment results of this airfoil which can be used for the calibration purposes. The designed model for the present tests had a span of 600 mm, which is equal to the width of the test section. The model chord is equal to 150 mm that results in h/c=4. There are 23 pressure taps on each side of the model that can scan the pressure distribution over both surfaces. The ports are located on a 30 degrees slanted line with respect to the model chord to provide more space for drilling and further to reduce the interaction between each port. In addition, in order to further investigate two dimensionality of the flow in the test section and on the model surface, eight pressure ports were located along the span of the model upper surface at four different locations. Figure 5 shows the schematic of the corresponding model as well as the pressure ports that are located on the upper surface in both chordwise and spanwise directions.

RESULTS AND DISCUSSION

After manufacturing the models, each of them were tested at various angles of attack and free stream Mach numbers for the calibration purposes. In the following sections, the results will be presented and compared with the available data, for various cases.

AGARD-B tests

The 3D model, illustrated in Figure 4 , was used to provide forces and moment data, L, D, P.M., and only one pressure port was used for the base pressure sensing. The model was tested at different free stream Mach numbers ranging from 0.51 up to 1. In each set of tests, the angle of attack was varied from -6 to 16 degrees with steps of 2 degrees and the corresponding forces and moment were recorded. The lift, forebody drag and pitching moment coefficients were then calculated, corrected, and are presented in Figure 6 and **Error! Reference source not found.**. The results are compared with the results of CSIR Laboratory, in South Africa (Ref.[7]), T-38 wind tunnel (Ref.[6]), AEDC (Ref.[1]), and NAL $4'\times4'$ trisonic wind tunnel (Ref.[8]).

In these tests, the effect of angle of attack on the aerodynamic forces and moment as well as the performance of the model; CL vs. CDf, was investigated. The results show that for Mach numbers below 0.73, the flow over the entire model surface is subsonic. For these cases, the wall porosity was zero, similar to the solid walls, hence no suction was applied. All data, except Cm vs. α, are compared with those of NAL and the comparisons are satisfactory. Further, Mach standard deviation of the measured data is lower than one percent, which is acceptable for this type of wind tunnel [[13]]. The slight difference between the present data and those of the NAL one are due to the Reynolds number and free stream turbulence. The differences in the acquired data are more pronounced for the CD and Cm data which are more sensitive to the free stream turbulence and Reynolds number. From these data, it is clearly seen that the deviation between the present data and those of various references for the lift case starts around $\alpha>12^0$ while for $\alpha<12^0$, the CL data compare excellently. For $\alpha>12^0$ apparently, the flow over a portion of the model is separated and as is known separation is a function of Reynolds number. Furthermore, free stream turbulence level has significant effect on the separation, too.

Aerodynamic forces and moment for other Mach numbers where the flow was fully subsonic are also acquired, but are not presented in this paper. From these data, it could be concluded that for these ranges of the free stream Mach numbers and for the 3D models, having the same blockage ratio as of the present one, there is no need for the side suction and the data could be used without much correction.

For higher free stream Mach numbers, $M_\infty>0.8$, both side suction and wall porosity must be applied to avoid choking and shock wave formation as well as the shock reflection from the wall over the model surface. The model is tested at $0.81<M_\infty<1$. For all cases, both side suction and porosity were applied and the data are compared with those of other tunnels. For similar cases as seen from **Error! Reference source not found.**, variations of CL vs. α and CL vs. CDF for $M_\infty=1$ are in good agreements with similar cases obtained from different tunnels except for those of the NAL tunnel. It is seen that CL vs. α data for the NAL tunnel for $M_\infty\approx1$ is slightly higher than the present data. Note that since the model is symmetric, upward shift of the data has no effect on the comparison of our data with NAL ones. In other word, since the model is symmetric, the CL vs. α curve must pass through the origin, CL=0 at $\alpha=0^0$. However, from the NAL tunnel data it is clearly seen that at $\alpha=0^0$, the CL is not equal to zero, **Error! Reference source not found.**a which is very important for the comparison. Thus, it seems that for low angles of attack, the slope of the CL vs. α diagram could be used as a comparison for all cases and as seen from **Error! Reference source not found.**a the values of CL_α, are in good agreement for all cases. However, the pitching moment data show larger deviations, **Error! Reference source not found.**c. This indicates that the applied suction and porosity of 2.5% for these cases are enough; however, the pitching moment data is affected by other parameter(s), i.e. Reynolds number, blockage for this Mach number, shock wave location etc., that needed to be further investigated.

After inspection, the problem was found to be related to the difference between Reynolds number of the present tunnel and that of the reference ones. ST2 is of a suction type wind tunnel while other tunnels are of blow down types with pressurized air that result in a much higher Reynolds number. At the same time, since the test section of ST2 is smaller than all other tunnels, smaller models can be tested in its test section and this will intensify the problem of low Reynolds number. For instance, the Reynolds number based on the mean chord of the model in ST2 was about 0.7×10^6 for $M_\infty=0.8$ while for other tunnels, the Reynolds number is in the order of 6 Million. Consequently, the boundary layer on the model is affected significantly and the normal shock location for $M_\infty\geq0.9$ is not the same. As a result, the pressure center is closer to the leading edge and the resulted pitching moment is smaller than the reported data.

From the above discussion, lift and drag coefficients for 3D tests are in a good agreement with the published data and it seems that no correction is needed. For high Mach numbers, $M_\infty>0.9$, however, correction should be applied and the correction factor has been calculated as a function of Mach number and angle of attack.

Because of large amount of acquired data from the tunnel, it was impossible to present all of them for all Mach numbers tested. A summary of the results are presented in Figure 8 through Figure 10 . Figure 8 shows the effect of free stream Mach number on the lift curve slope of the AGARD-B model for the linear range of CL vs. α data. The data for a few other tunnels are shown for comparison. The figure shows that for all cases, the lift curve slope of the model increases with increasing the free stream Mach number up to a Mach number of about 0.95, where it reaches its maximum value. For higher Mach numbers, $M_\infty>0.95$, the lift curve slope decreases with

increasing the free stream Mach number, Figure 8 . Comparison between the present data and those of the reference ones from NAL and AEDC wind tunnel shows that the acquired data, lies within the scatter of referenced data. The slight differences are due to the Reynolds number, surface roughness, shock location, blockage effect, instrument error, etc.

Figure 9 shows variation of the fore body drag coefficient at zero degree angle of attack versus free stream Mach number. From this figure it is clearly seen that again the presented data are in good agreement with those of other tunnels for similar cases. Further, this figure shows that the value of CDf at zero lift coefficient, CL=0, is almost constant up to $M_\infty \approx 0.95$. For higher Mach numbers, CDf increases, reaching its maximum value at $M_\infty \approx 1.1$. This increase in CDf is of course related to the formation of normal shock waves somewhere over the model surface where its strength increases as the free stream Mach number is further increased. For Mach numbers higher than 1.2, it is expected that CDf decreases since the normal shock will move forward toward the tip of the nose and becomes an oblique shock. The losses through an oblique shock wave are much less than the corresponding one through a normal shock, thus it is expected that CDf will decrease at higher Mach numbers, $M_\infty > 1.2$.

Figure 10 shows the effect of free stream Mach number on the pitching moment stability derivative ($C_{m\alpha}$). According to the diagram, $|C_{m\alpha}|$ is a monotonically decreasing as the free stream Mach number is increased up to $M_\infty \approx 0.9$. However, the model is stable even at sonic speed, $M_\infty \approx 1$, but the stability margin decreases as the free stream Mach number is increased. This figure again shows that the results are in good agreement with those of NAL tunnel.

Figure 10 shows that in the vicinity of $M_\infty \approx 0.925$, $|C_{m\alpha}|$ decreases sharply and then remains almost constant with further increasing M_∞, $M_\infty > 0.93$. This Mach number, $M_\infty \approx 0.925$ is the same Mach number where CDf rises sharply, Figure 9 . Thus it could be concluded that the free stream Mach number of $M_\infty \approx 0.925$, is drag divergence Mach number for this model under this condition. Beyond this Mach number, $M_\infty \approx 0.925$, the position of normal shock, apparently does not vary significantly with increasing the free stream Mach number, Figure 10 , however, its strength will increase, Figure 9 .

NACA0012 tests

The 2D NACA0012 airfoil model, discussed previously, was used to measure its surface static pressure distribution to investigate the effects of porosity and side suction on its aerodynamic derivatives and to further study the effectiveness of these parameters on the wind tunnel operation in the transonic regime. The designed and manufactured model had a span of 600mm which is equal to the wind tunnel test section width and had a chord of about 150mm that results in the test section height to chord ratio of about 4. Pressure port arrangement was discussed in the model description section. The designed and manufactured model was tested at different free stream Mach numbers, ranging from $M_\infty = 0.4\text{-}0.95$, and the angle of attack was varied from zero to 4 degrees. Surface pressure distribution on both upper and lower surfaces of the airfoil as well as the schlieren pictures are presented in this paper.

An important problem in the transonic tests is related to the sensitivity of the shock location and transition point due to the flow variables i.e. precision of the free stream Mach number setting, Reynolds number, surface roughness, turbulence level of the tunnel and even acoustic level. For instance, the pressure distribution on the NACA0012 airfoil in two different wind tunnels of the NASA Langley is illustrated in Figure 11 for the same Reynolds numbers of about 2.1 Million. As seen from this figure, shock location in different wind tunnels varies up to 15% of the model chord. The location of the shock wave from the Cp data is where there is a jump, increase in |Cp|, as illustrated in Figure 11 a. In this figure, note that for $\Delta M_\infty = 0.003$, the shock wave location varies about $\Delta x/C \approx 0.15$. In addition, when the tests are repeated, the shock location may vary too, $\Delta x/C \approx 0.05$ as seen from Figure 11 a. Figure 11 b shows similar trend, too. The redundancy of the tests in the transonic regime is another problem which is due to the occurrence of the shock wave on the model surface and high sensitivity of the shock location with other variables.

The presented results are compared with the published data of ATA, Langley wind tunnels (4 by 18 inch and 6 by 19 inch) and the results from Ref [9]. The experimental results for the zero degrees angle of attack are shown in Figure 12 through Figure 14 and are compared with the available experimental data from other wind tunnels.

Figure 12 shows variations of the pressure coefficient with x/c for the lowest possible free stream Mach number in this wind tunnel, $M_\infty = 0.4$, at zero degrees angle of attack. The data are compared with those of NASA Langley tunnel and the computational results obtained by the code that was developed by the authors [[9]]. This figure indicates that the experimental data are in excellent agreement with the previous findings as well as the present computational one.

Effect of Mach number on the surface pressure distribution of the NACA 0012 model is shown in Figure 13 and Figure 14 for $0.73 \le M_\infty \le 0.91$ at zero degrees angle of attack and for a tunnel porosity of 2.5 percent with the suction on case. Note that this porosity was set in the vicinity of the model. Far from the model, the porosity was zero. Again, the data for all Mach numbers are compared with the available experimental data and as seen from the figures, present data are in good agreement with the available ones. Shadowgraph photos of the model with the shock wave located on both surfaces are shown in each figure, too. As the free stream Mach number increases, the shock wave becomes stronger and moves further away from the leading edge. Effect of increasing the free stream Mach number can be clearly seen from the jump in the |Cp| value, |Cp| decreases suddenly at the shock location over the surface of the model, Figure 12 to Figure 14 . By careful examination of these figures, one can clearly realize the sensitivity of the surface

pressure with the variations of the free stream Mach number. In addition, from these figures it is clearly seen that the present Cp data with the aforementioned test conditions compares excellently with the available experimental data for $\frac{x}{C}$'s from the leading edge until the point where the shock wave is located which varies with the free stream Mach numbers. At $\frac{x}{C}$'s where the shock is located, Cp data differs slightly which could be the result of many parameters, i.e. Reynolds number, free stream Mach number, suction, etc. However, as was seen from Figure 14 , the pressure distribution for the referenced tunnel varies too and by careful inspection of Figure 12 to Figure 14 it is clearly seen that that the differences between the present Cp data and those of the other tunnels are much less than those presented in Figure 11 .

Figure 14 shows the pressure distribution on the model surface for M∞=0.91 and as seen from this figure, the present data are close to those from the Langley and ATA findings. Moreover, the schlieren photo shows no shock reflection from the upper and lower walls that indicates the effectiveness of the porosity and side suction from the test section walls. From the Cp data, it is apparent that the shock location on the model surface for this Mach number is about 0.74 of the chord that is in good agreement with the reference data of Langley.

Figure 15 from Ref [[12]] shows the effects of free stream Reynolds number on the shock position for NACA0012 airfoil when tested at $M_\infty = 0.81$. The data are for various wind tunnels all over the world. The present data is also included in this figure. As seen from this figure, the scatter of the data is significant which is due to the various sources mentioned previously. For the present test, as mentioned in the article, the acceptable range of shock wave location for this airfoil when tested at M∞=0.8 and α=0 deg is $\frac{x}{C} = 0.46 \pm 0.02$. As seen from Figure 15 the present data lies within the acceptable range which indicates that the operation of the tunnel with the applied side suction is acceptable.

Figure 16 shows the effect of angle of attack and free stream Mach number on the normal shock location over the airfoil. In addition, the data are compared with the available data from other tunnels. Seen from this figure the acquired data in the tunnel for angle of attack of two degrees are also in good agreement with those of other tunnels. The results for other Mach numbers and also for angle of attack of 4 degrees, show similar trends.

CONCLUSION

Intensive experiments over both 2-D and 3-D calibration models were performed to investigate the flow improvements and performance of an upgraded transonic wind tunnel. Surface pressure data over the 2-D model at various free stream Mach numbers and angles of attack in the subsonic through transonic regimes were obtained and compared with the existing data of other tunnels for the similar cases. From these comparisons it was concluded that the data of the upgraded tunnel in the transonic regime is reliable when surface porosity and enough suction is applied. Similar results were obtained for the 3-D model. However, the pitching moment data of the 3-D model did not compare excellently. Therefore, further investigations are needed to find and fix this problem. However, other data, lift and drag (CDf) compare excellently. The discrepancy of the pitching moment is in the acceptable range, while the authors expect better accuracy. In conclusion, with the aforementioned changes in the present wind tunnel, the acquired data in the transonic regime are accurate and one can use them if right conditions and corrections are met.

FIGURES

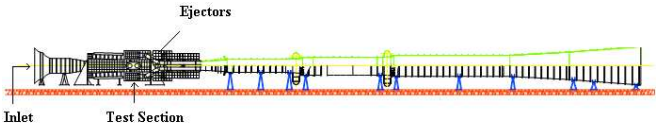

Figure 1 ST2 Wind tunnel main circuit

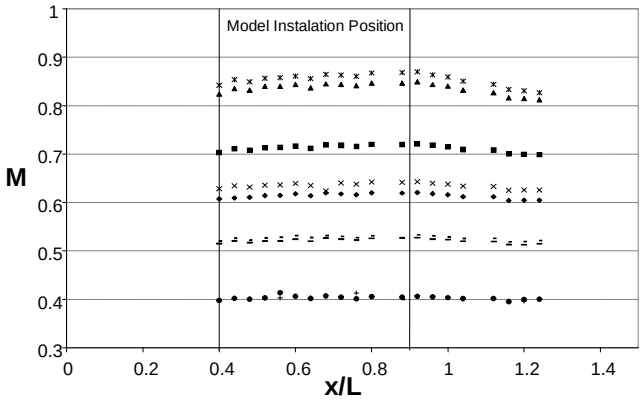

Figure 2 Mach number distribution along the centerline of the test section, closed walls

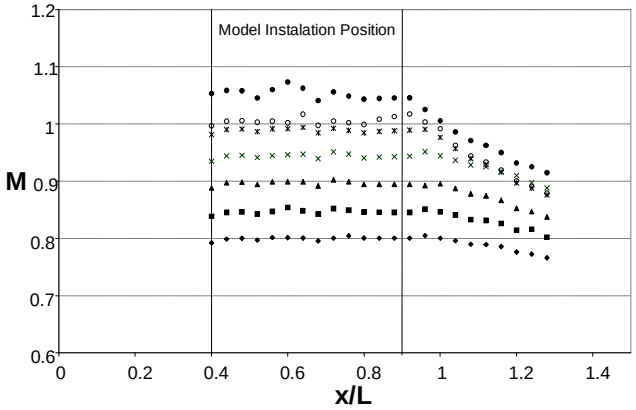

Figure 3 Mach number distribution along the centerline of the test section, normal perforated walls

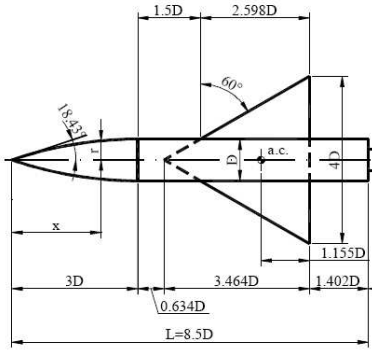

Figure 4 Basic dimensions of the AGARD-B model

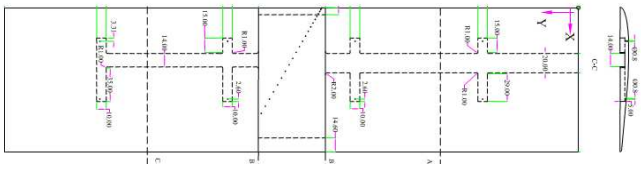

Figure 5 Schematic of the 2D model

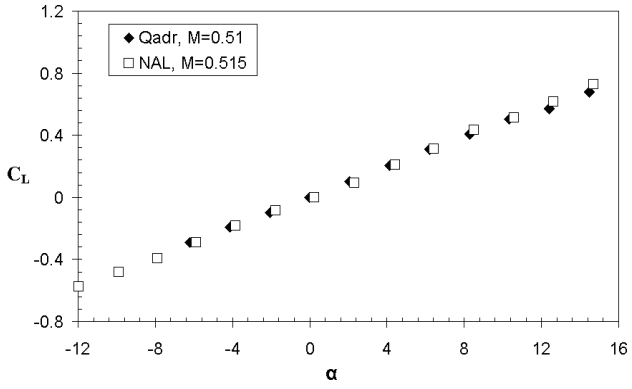

a) C_L Vs. α

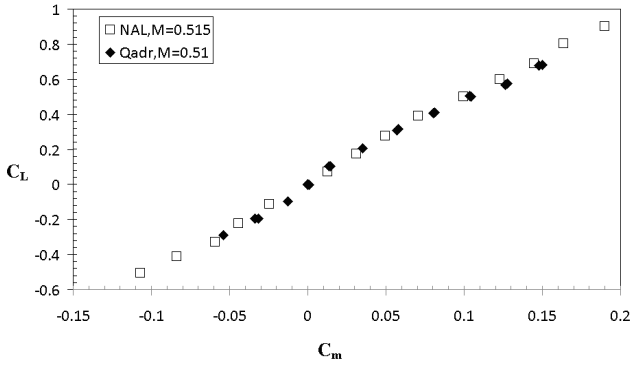

b) C_L Vs. C_m

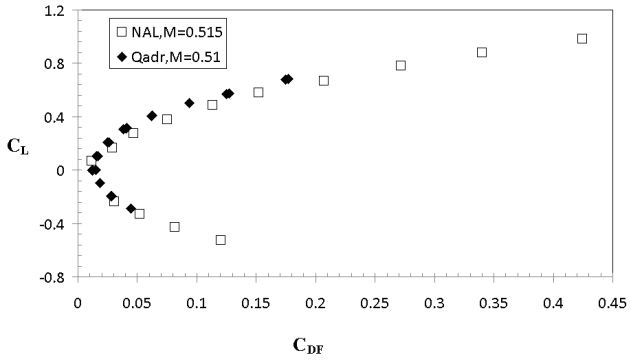

c) C_L Vs. C_{DF}

Figure 6 Force and moment results for AGARD-B model, M=0.515, no porosity.

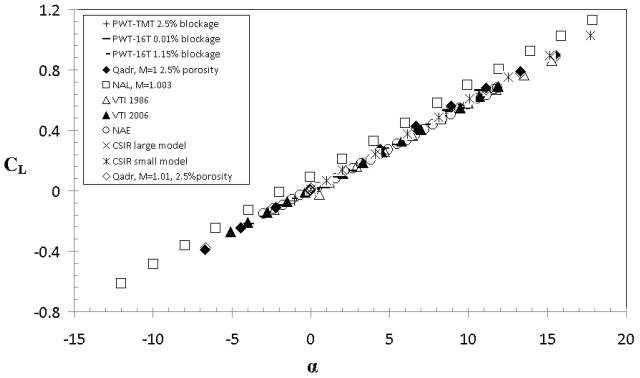

a) C_L Vs. α

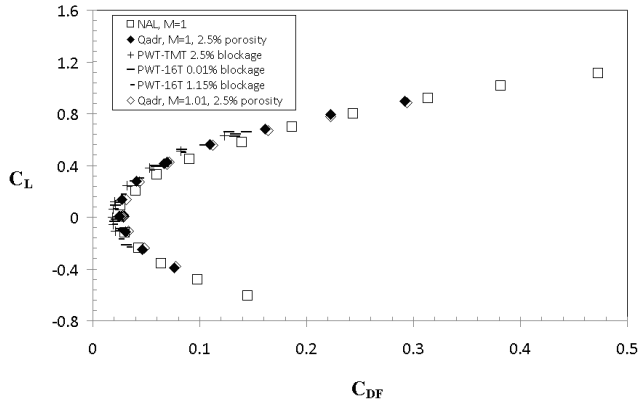

b) C_L Vs. C_{DF}

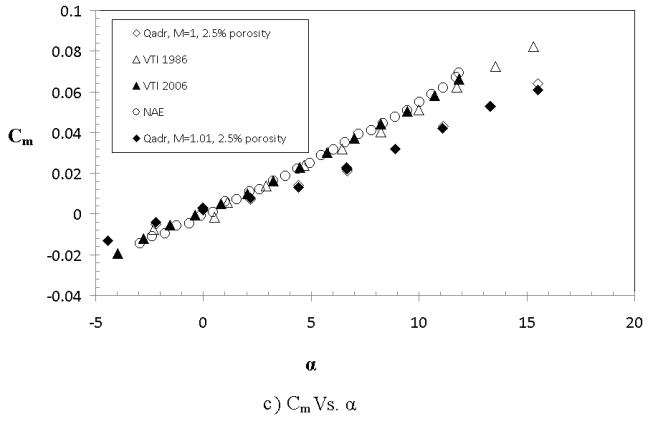

c) C_m Vs. α

Figure 7 Force and moment results for AGARD-B model, M=1, porosity=2.5%, with side suction

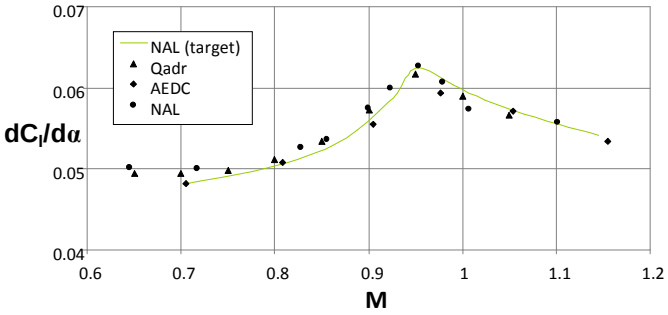

Figure 8 Lift curve slope Vs. M for AGARD-B model

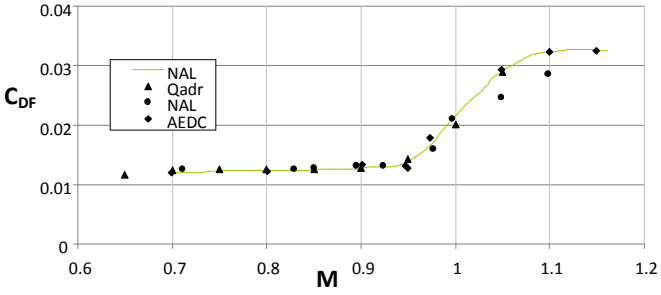

Figure 9 Forebody drag coefficient at at CL=0 Vs M for AGARD-B model

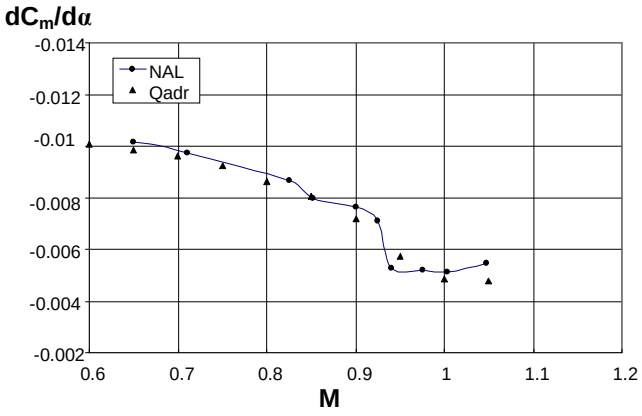

Figure 10 $\partial Cm/\partial \alpha$ Vs. M for AGARD-B model

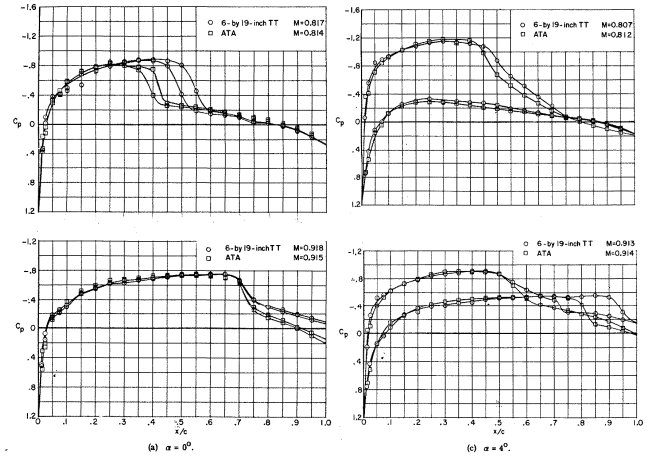

Figure 11 Pressure distribution over NACA-0012 airfoil at two different wind tunnels [[10]]

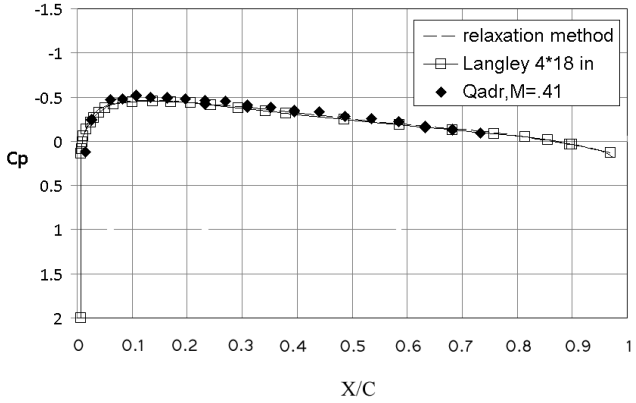

Figure 12 Pressure distribution over NACA 0012 at M=0.4, porosity=0, α=0

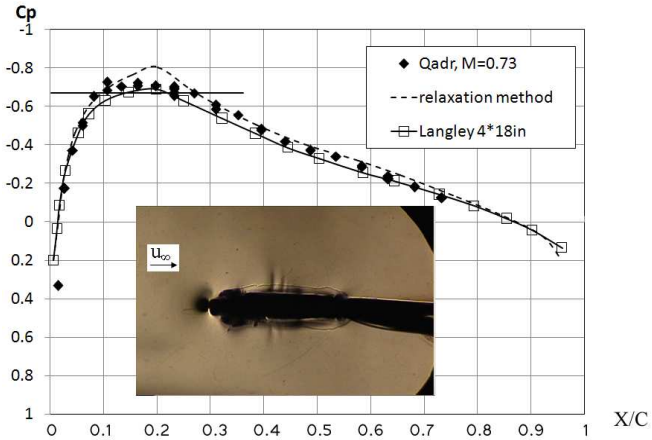

Figure 13 Pressure distribution over NACA 0012 at M=0.73, porosity=2.5%, α=0, with suction

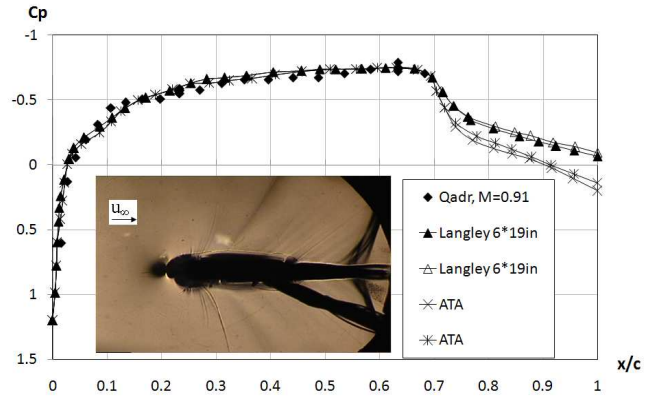

Figure 14 Pressure distribution over NACA 0012 at M=0.91, porosity=2.5%, α=0, with suction

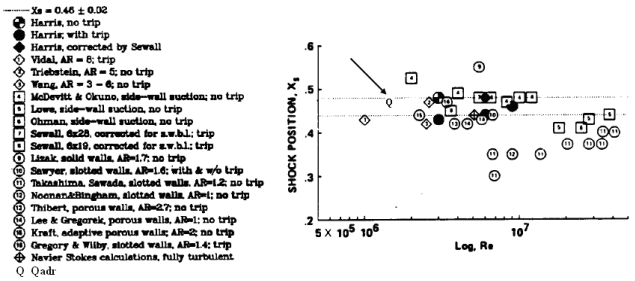

Figure 15 Shock location on NACA-0012 airfoil in different wind tunnels in M=0.81.

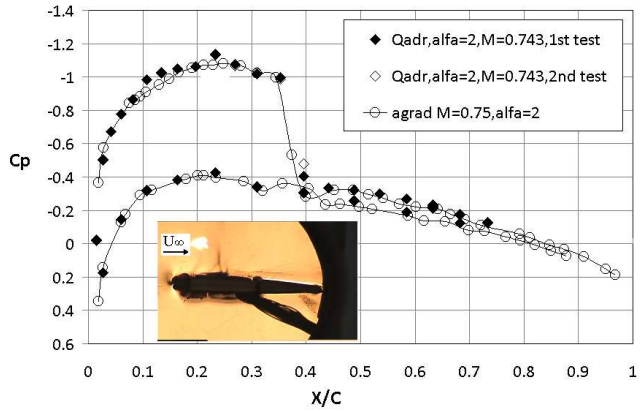

Figure 16 Pressure distribution over NACA 0012 at M=0.74 and at alfa=2

REFERENCES

[1] B. H. Goethert, "*Transonic Wind Tunnel Testing*", Pergamon Press, New York, 1961.

[2] A. Pope and K. L. Goin, "*High speed wind tunnel testing*", Robert E. Krieger Publishing Company, New York, 1978.

[3] J. L. Grunnet, "Transonic Wind Tunnel Wall Interference Minimization, Fluid Dynamics Engineering Corporation", Minneapolis, Minnesota, AIAA, September, 1984.

[4] N. Ulbrich and A. R. Boone, "Validation of a Wall Interference Correction System for a Transonic Wind Tunnel", NASA Ames Research Center, California 94035(1000), AIAA 2004-605.

[5] D. J. William," Optimization of Wave Cancellation in Variable Porosity Transonic Wind Tunnel Flows", George C. Marshall Space Flight Center, Alabama 35812, 1973.

[6] D. Damljanović, A. Vitic, and D. Vukovic, "Testing of AGARD-B Calibration Model in the T-38 Trisonic Wind Tunnel", Scientific-Technical Review, Vol. LVI, No .2, 2006.

[7] G. Lombardi, and M. Morelli, "Analysis of Some Interference Effects in a Transonic Wind Tunnel", Journal of Aircraft, Vol. 32, No. 3, May-June 1995.

[8] H. C. Seetharam, and R. Rangaflajan, "Force Calibration of AGARD-B Model in Transonic Flow Mach Numbers", National Aeronautical Laboratory, Bangalore, Technical Memorandum, NO.TM-PR. 200/69-70.

[9] J. L. Amick, "Comparison of the Experimental Pressure Distribution on a NACA 0012 Profile at High Speeds With That Calculated by the Relaxation Method", Langley Aeronautical Laboratory, TN. 2174.

[10] Ladson, C. L., 1973, "Description and calibration of the Langly 6-by-19 inch transonic tunnel", NASA Langley research center, NASA TN D-7182.

[11] Amiri K., Soltani M. R., "Exprimental Investigation of Effects of Suction and Wall Porosity on Flow Quality in a Transonic Wind Tunnel", Aerotech III 2009, AER009, University Putra-Malaysia, 17-19 Nov 2009.

[12] McCroskey, W. J., 1987, "A Critical Assessment of Wind Tunnel Results for the NACA0012 Airfoil", NASA Technical Memorandum 100019, TR 87-a-5.

[13] Amiri K., Soltani M. R., Haghiri A., Mani M.," *An Investigation on the Effects of Wall Porosity and Side Suction in Transonic Tests*" Journal of Aerospace science and Technology (JAST), Vol. 6, No. 2, PP 63-70 (2009).